Chapter 2
Research on Gearbox Fault Diagnosis of Urban Rail Vehicle Based on SIMPACK

Xiukun Wei, Dong Yan and Jun Chen

Abstract Gearbox, an important component of urban rail vehicles working in the most severe conditions, plays a crucial role in the urban rail vehicle fault diagnosis. It is necessary to detect the fault of gearbox at an early stage to prevent human casualties and reduce maintenance costs. Most of the data-driven fault diagnosis methods are based on an experimental platform, which has many disadvantages such as costly maintenance, limited application, and limited degree of fault simulation. In this paper, a new method based on SIMPACK is proposed and confirmed efficient by testing, which can overcome the disadvantages of the experimental platform. Meanwhile, MATLAB was applied to time–frequency domain analysis and wavelet packet analysis. These analysis results demonstrated the feasibility and reliability of this method.

Keywords Gearbox · SIMPACK · Fault diagnosis · Time–frequency domain analysis · Wavelet packet analysis

2.1 Introduction

Gearbox is a dispensable component of urban rail vehicle, and it is the place where fault occurs easily. According to statistics, 60 % of the gearbox fault occurred on gear, 19 % occurred on shaft [1], and all of the faults interact with each other.

X. Wei (✉) · D. Yan · J. Chen
State Key Laboratory of Rail Traffic Control and Safety, Beijing Jiaotong University, Beijing, China
e-mail: xkwei@bjtu.edu.cn

X. Wei · D. Yan
Shanghai Key Laboratory of Computer Software Evaluating and Testing (Shanghai Development Center of Computer Software Technology), Shanghai, China

Y. Qin et al. (eds.), *Proceedings of the 2015 International Conference on Electrical and Information Technologies for Rail Transportation*, Lecture Notes in Electrical Engineering 378, DOI 10.1007/978-3-662-49370-0_2

The faults must be detected at an early stage to reduce maintenance costs, improve productivity, increase machine availability, and prevent human casualties [2].

With the rapid progress of modern testing and signal processing technology, researchers pay more and more attention to vibration analysis. Successful examples of fault diagnosis can be found in [3]. The literature [4] has detailed works on the implementation process of wavelet analysis and application in fault diagnosis. Time–frequency approach recognition of faults in gear tooth is presented in the literature [5]. A PCA improved algorithm of BP neural network is introduced in paper [6]. The data-driven methods that describe the above are based on an experimental platform, which has many disadvantages. In this paper, a new method based on SIMPACK is proposed for overcoming the disadvantages and achieving a fundamental change in the condition-based monitoring and fault diagnosis of gearbox.

The rest of this paper is organized as follows. In Sect. 2.2, gearbox modeling is introduced. Section 2.3 describes three kinds of gearbox faults which is analyzed by time–frequency domain. In Sect. 2.4, taking shaft-misalignment is analyzed by wavelet. The conclusions are drawn in Sect. 2.5.

2.2 Modeling of Gearbox

Parameters from ZMA080 of metro vehicle were chosen for the model. The density of gearbox case is 7.3 g/cm^2, involute helical gears is adopted by the driver gear and passive gear [7]. Simulation time is 20 s and sampling frequency is 24 kHz. Two sensors were installed at holding point of gearbox and the data in the first 5 s were removed during analysis. Parameters of gear and motor are shown in Tables 2.1 and 2.2, respectively. The basic parameters of gearbox are presented in Table 2.3. Detailed parameters setting is shown in Fig. 2.1, which is a topology graphics of gearbox. The 3-D dynamic model based on SIMPACK is shown in Fig. 2.2.

Table 2.1 Parameters of gear

Name	Normal modulus	Gear number (driver)	Gear number (passive)	Tooth profile angle	Helix angle
Value	5	19	120	20°	12.2°

Table 2.2 Basic technical parameters of the motor

Name	Rated power	Rated speed	Max speed	Starting torque	Rated torque	Max traction torque
Value	190 kW	1800 r min^{-1}	3481 r min^{-1}	1625 N m	1008 N m	1626 N m

Table 2.3 Basic parameters of gearbox

	Case body		Input shaft	Output shaft		Driver gear		Passive gear	
Size/mm	656 * 1005 * 286		L: 400	L: 400		Addendum D: 107		Addendum D: 624	
			R: 60	R: 60		Root circle D: 85		Root circle D: 601	
Mass/kg	127.6		31.5	7.3		1		1	
Rotational inertia/kg m^2	Ix	5.45	Ix	0.054	0.0029	Ix	1	Ix	1
	Iy	11.61	Iy	0.448	0.0993	Iy	1	Iy	1
	Iz	15,032	Iz	0.448	0.0993	Iz	1	Iz	1

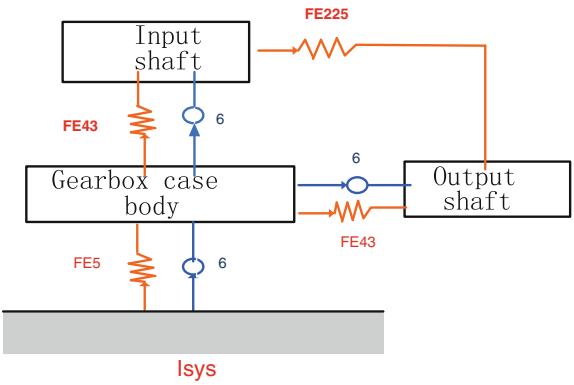

Fig. 2.1 Topology of gearbox model

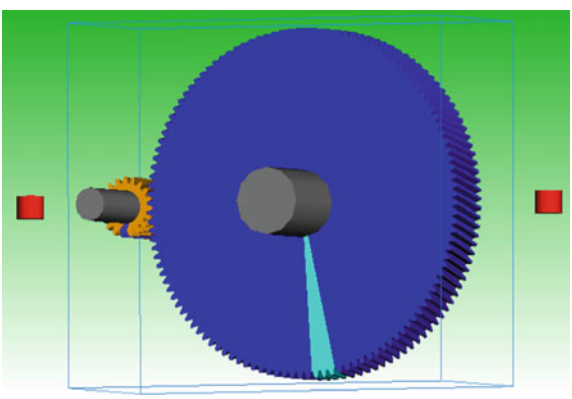

Fig. 2.2 3-D dynamic model of gearbox

2.3 Fault Diagnosis of Gearbox

2.3.1 Symmetrical Tooth Wear Analysis

The comparison of time domain waveform of acceleration signal between normal and symmetrical tooth wear can be found in Fig. 2.3, where the amplitude of acceleration is aggravated when symmetrical tooth wear occurs. The characteristic, which is presented in Fig. 2.4, shows that peaking and kurtosis change greatly. Amplitude spectrum of axial force has shown that meshing frequency and double meshing frequency increased when symmetrical tooth wear occurred in Fig. 2.5.

According to the results, the conclusions of symmetrical tooth wear are [8]:

- Energy of vibration increases when tooth wear occurs (including effective value and other indexes).
- Amplitude of meshing frequency and doubling frequency aggravates.

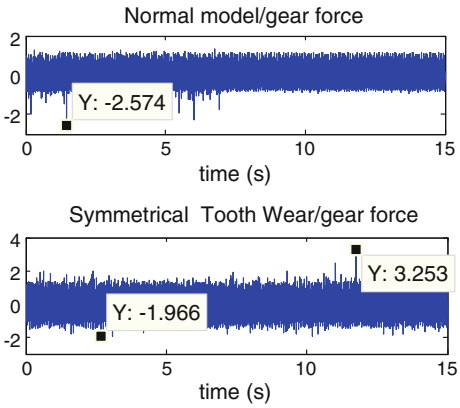

Fig. 2.3 Time domain signal of acceleration

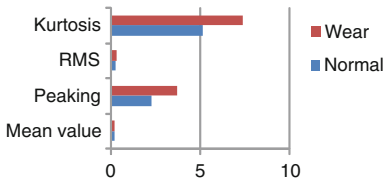

Fig. 2.4 Time domain characteristic

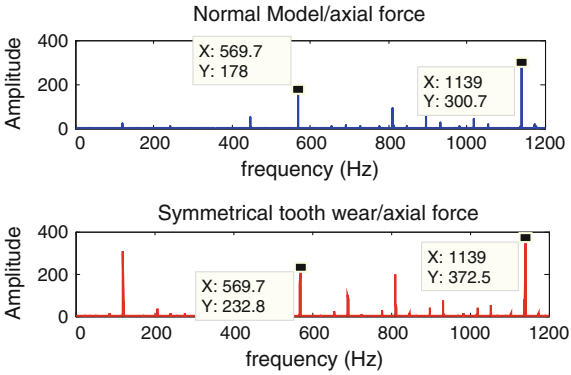

Fig. 2.5 Amplitude spectrum comparison chart of axial force

2.3.2 *Shaft Misalignment Analysis*

In Fig. 2.6, time domain waveform comparison of axial force shows that the range of axial force changes greatly and impulsive periodic signal occurs, which is the most significant difference. The gears cannot mesh with others when the shaft misalignment occurs as shown in Fig. 2.7; it also explains the phenomenon of impacted periodicity signal. The change in peak value is much higher than the other characteristics in Fig. 2.8.

Amplitude spectrum is shown in Fig. 2.9, the axial force of normal model concentrates on meshing frequency and double meshing frequency entirely, and axial force of shaft-misalignment model concentrates on rotation frequency and also its double frequency. The amplitude of failure model is higher than normal in Fig. 2.10. In addition, the carry wave frequency of the sideband, which is generated by failure model, is meshing frequency and its harmonics, and the model created fault shaft rotation frequency and double rotation frequency for interval of sideband clearly.

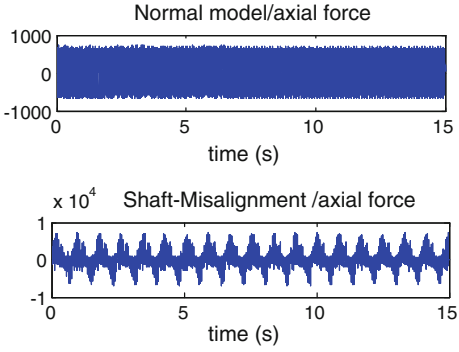

Fig. 2.6 Time domain waveform of axial force

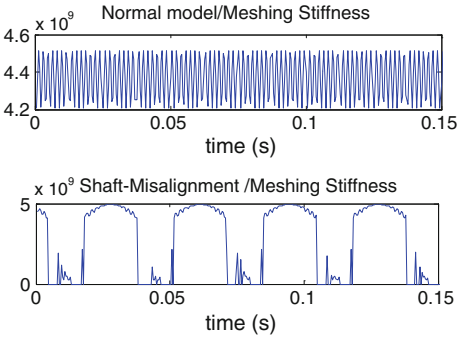

Fig. 2.7 Chart of meshing stiffness

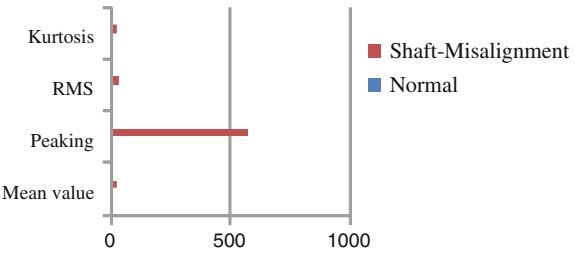

Fig. 2.8 Characteristic value of shaft misalignment

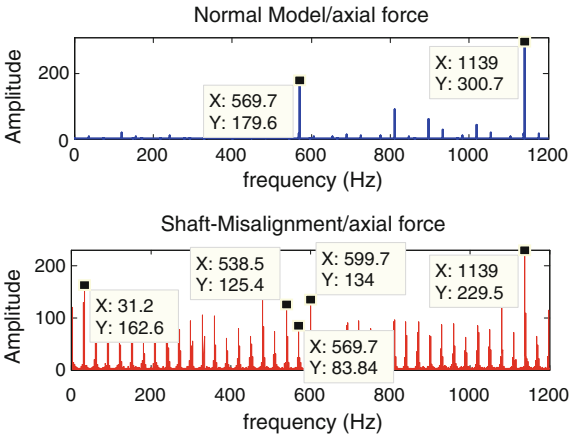

Fig. 2.9 Amplitude spectrum of axial force

According to the results, the conclusions of shaft misalignment are [8]:

- Generating sideband, which is centered by meshing frequency and double meshing frequency and its intervals are rotation frequency and double rotation frequency.
- Amplitude of frequency and double meshing frequency is higher than the normal.
- Energy of vibration increases when shaft misalignment occurs (including effective value and other characteristic values).

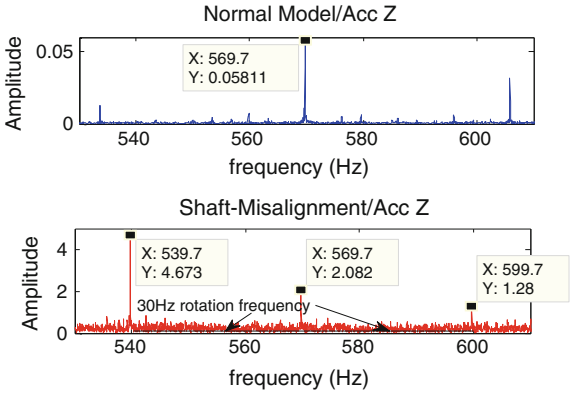

Fig. 2.10 Amplitude spectrum comparison chart of acceleration signal (z direction)

2.3.3 *Mild Bending of Shaft Analysis*

What meshing stiffness comparison Fig. 2.11 shows is a periodic change when mild bending of shaft occurs. Characteristic values are shown in Fig. 2.12, the peak value and kurtosis increase greatly in all the characteristic values.

For further analysis, increasing amplitude that corresponds to rotation frequency of fault shaft is shown in Fig. 2.13, and the carry wave frequency of the sidebands, which is generated by failure model, is meshing frequency and its harmonics. Rotation frequency of input shaft is 30 Hz, transmission ratio is 6.32, rotation frequency of output shaft is 4.7 Hz, and double frequency is 9 Hz when input shaft is failure. Amplitude spectrum comparison chart of axial force is presented in Fig. 2.14, where meshing frequency and double meshing frequency are clear.

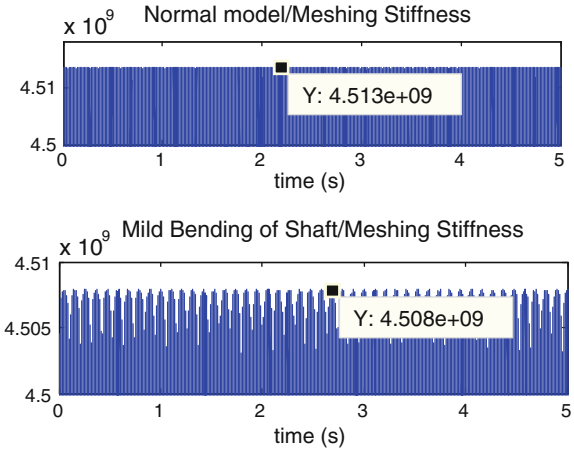

Fig. 2.11 Comparison of meshing stiffness

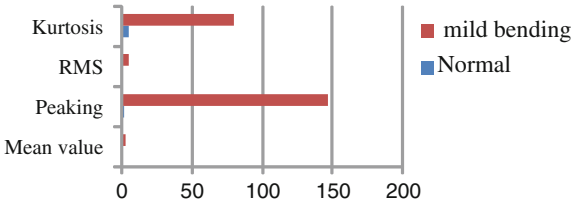

Fig. 2.12 Characteristic value of shaft misalignment

Fig. 2.13 Acceleration signal amplitude spectrum

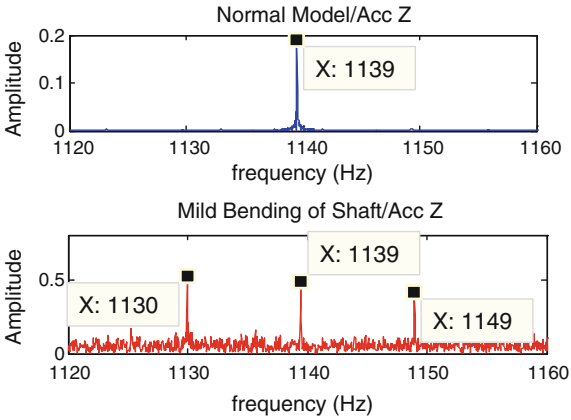

Fig. 2.14 Amplitude spectrum of axial force

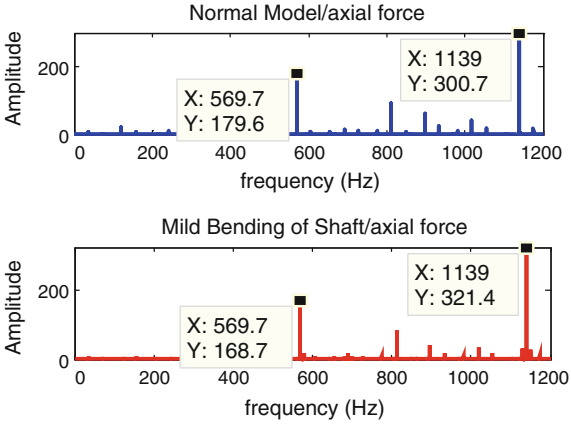

According to the results, the conclusions of mild bending of shaft are [8]:

- Amplitude of meshing frequency and double frequency increases significantly.
- Gearbox system generates sidebands around the meshing frequency, and the meshing frequency and its harmonics are frequencies of carry wave when mild bending occurs.

- Energy of vibration increases when mild bending of shaft occurs (including effective value and other characteristic values).

2.4 Wavelet Analysis

A partially magnified point S30 is shown in Fig. 2.15 (1), and the wavelet packet decomposition of vibrating signal is shown in Fig. 2.16 (2). Vibration intensity of each fault model layer is higher than normal layer, especially point S30. The phenomenon is caused by low frequency of 30 Hz of fault shaft rotation frequency.

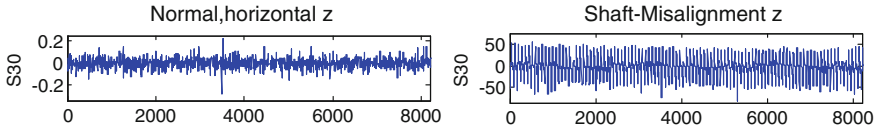

Fig. 2.15 Wavelet packet decomposition of vibrating sign (1)

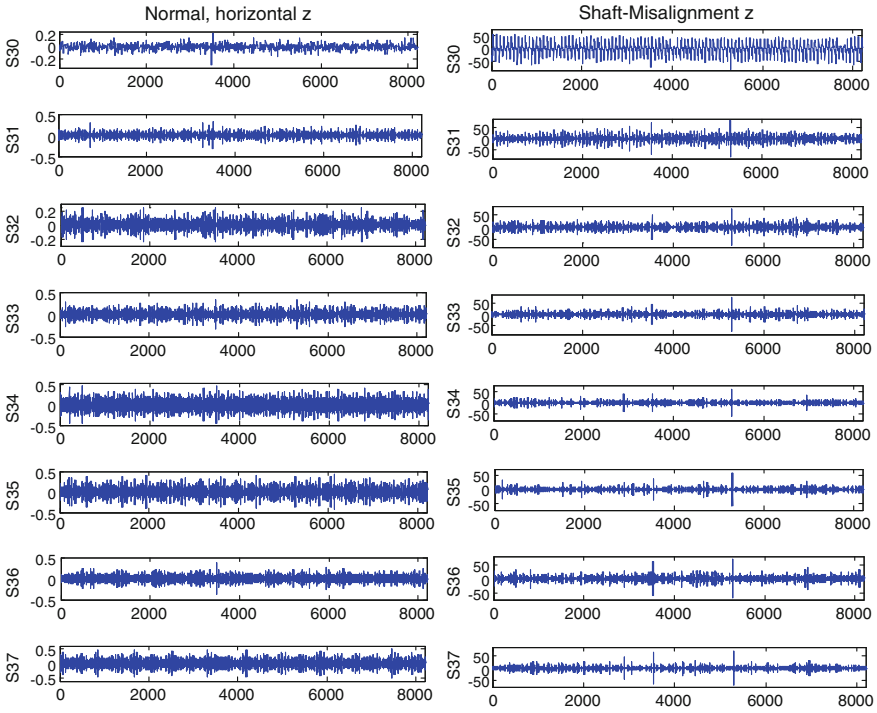

Fig. 2.16 Wavelet packet decomposition of vibrating sign (2)

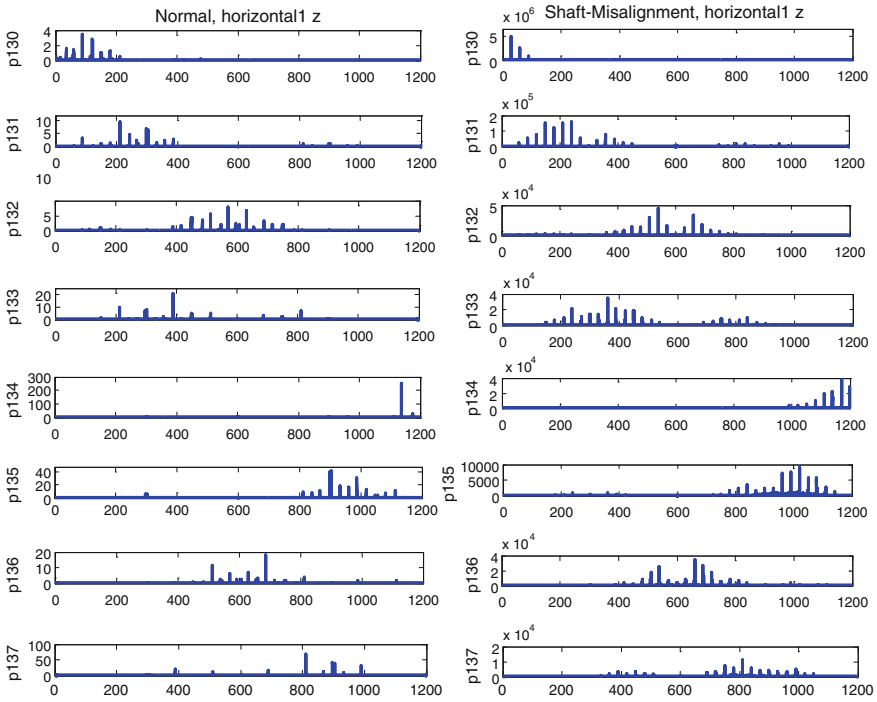

Fig. 2.17 Power spectrum of each layer signal of vibrating signal

From power calculation and analysis of signal of each layer, it is shown that the power of shaft-misalignment signal is far higher than the power of normal signal. The phenomenon is caused by increased vibration of the gear system when failure happens, and the results are shown in Fig. 2.17.

The energy distribution histograms of signal of each layer are shown in Figs. 2.18 and 2.19. It can be seen that the energy of normal model mainly concentrates on meshing frequency and double meshing frequency; in other words, higher frequency energy accounts for a larger proportion in the total energy. Energy of rotation frequency of shaft misalignment increases greatly, its rotation frequency is 30 Hz, which belongs to low frequency band 0–300 Hz, and the low frequency band energy accounts for nearly 60 % of the total energy.

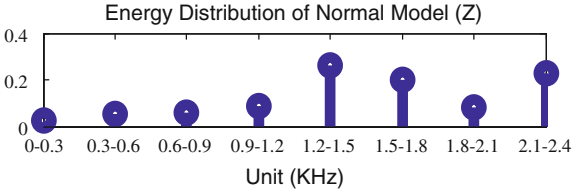

Fig. 2.18 Energy distribution of normal

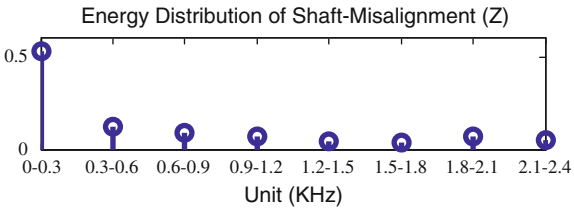

Fig. 2.19 Energy distribution of axle misalignment

2.5 Conclusions

In this paper, simulation based on SIMPACK is introduced, and the applicability of the method is verified by calculations and analyses. The conclusions in this paper are similar to gearbox analysis book [8]. Further extension of this work is under way to concentrate on more kinds of gearbox faults, such as pitting, broken, and invalidation. Additional suggested lines of work can be done on gearbox fault feature extraction techniques and methods. In this way, the method of fault diagnosis provided by SIMPACK will be more accurate and flexible.

Acknowledgments This work is partly supported by Shanghai Key Laboratory of Computer Software Evaluating and Testing (Grant number: SSTL2015_01), Chinese National Key Technologies R&D program (Contract No. 2015BAG13B01) and State Key Laboratory of Rail Traffic Control and Safety (Contract No. RCS2014ZZ005).

References

1. Lan F (2006) Study on diagnosis of typical gear faults. Sichuan Metall 28:47–48 (in Chinese)
2. Li B, Zhang P, Tian H, Mi S, Liu D, Ren G (2011) A new feature extraction and selection scheme for hybrid fault diagnosis of gearbox, Expert Syst App 38:10000–10009
3. Dempsey PJ (2008) Integrating oil debris and vibration gear damage detection technologies using fuzzy logic. In: NASA, US
4. Inalpolat M, Kahraman A (2009) A theoretical and experimental investigation of modulation sidebands of planetary gear sets. J Sound Vibr 323:677–696
5. Meltzera G, Dienb NP (2004) Fault diagnosis in gears operating under non-stationary rotational speed using polar wavelet amplitude maps. Mech Syst Signal Process 18:985–992
6. Kong Q, Huang F (2011) Research of gearbox fault diagnosis based on the PCA—improved algorithm of BP neural network. Instrum Technol 9:16–19 (in Chinese)
7. Pu Q, Zhou J (2011) Bogie gear box development of metro vehicle ZMA080 of Type A. Electr Locomotives Mass Transit Veh 4(34) (in Chinese)
8. Ding K, Li W, Zhu X (2006) Practical technology of fault diagnosis of gear and gear box. China Machine Press, Beijing (in Chinese)

http://www.springer.com/978-3-662-49368-7

Proceedings of the 2015 International Conference on Electrical and Information Technologies for Rail Transportation
Transportation
Qin, Y.; Jia, L.; Feng, J.; An, M.; Diao, L. (Eds.)
2016, XXVI, 801 p. 278 illus. in color., Hardcover
ISBN: 978-3-662-49368-7